Journal of Medicinal Chemistry

ARTICLE

pubs.acs.org/jmc

Synthesis, Biological Evaluation, and Automated Docking of Constrained Analogues of the Opioid Peptide H-Dmt-D-Ala-Phe-Gly-NH_2 Using the 4- or 5-Methyl Substituted 4-Amino-1,2,4,5-tetrahydro-2-benzazepin-3-one Scaffold

Rien De Wachter,[†] Chris de Graaf,[*,†,§] Atilla Keresztes,[∥] Bart Vandormael,[†] Steven Ballet,[†] Géza Tóth,[∥] Didier Rognan,[‡] and Dirk Tourwé[*,†]

[†]Department of Organic Chemistry, Vrije Universiteit Brussel, Pleinlaan 2, B-1050 Brussels, Belgium

[‡]Structural Chemogenomics, UMR 7200 CNRS-UdS, Université de Strasbourg, Illkirch F-67401, France

[§]Leiden/Amsterdam Center for Drug Research, Division of Medicinal Chemistry, Faculty of Science, VU University Amsterdam, Amsterdam, The Netherlands

[∥]Institute of Biochemistry, Biological Research Centre, Hungarian Academy of Sciences, Szeged, Hungary

Supporting Information

ABSTRACT: The Phe[3] residue of the N-terminal tetrapeptide of dermorphin (H-Dmt-D-Ala-Phe-Gly-NH_2) was conformationally constrained using 4- or 5-methyl-substituted 4-amino-1,2,4,5-tetrahydro-2-benzazepin-3-one (Aba) stereoisomeric scaffolds. Several of the synthesized peptides were determined to be high affinity agonists for the μ opioid receptor (OPRM) with selectivity over the δ opioid receptor (OPRD). Interesting effects of the Aba configuration on ligand binding affinity were observed. H-Dmt-D-Ala-*erythro*-(4*S*,5*S*)-5-Me-Aba-Gly-NH_2 **9** and H-Dmt-*threo*-(4*R*,5*S*)-5-Me-Aba-Gly-NH_2 **12** exhibited subnanomolar affinity for OPRM, while they possess an opposite absolute configuration at position 4 of the Aba ring. However, in the 4-methyl substituted analogues, H-Dmt-D-Ala-(4*R*)-Me-Aba-Gly-NH_2 **14** was significantly more potent than the (4*S*)-derivative **13**. These unexpected results were rationalized using the binding poses predicted by molecular docking simulations. Interestingly, H-Dmt-D-Ala-(4*R*)-Me-Aba-Gly-NH_2 **14** is proposed to bind in a different mode compared with the other analogues. Moreover, in contrast to Ac-4-Me-Aba-NH-Me, which adopts a β-turn in solution and in the crystal structure, the binding mode of this analogue suggests an alternative receptor-bound conformation.

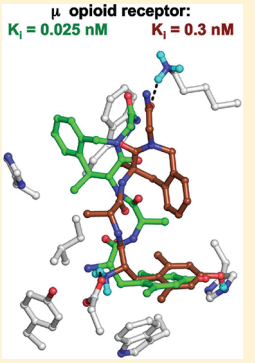

INTRODUCTION

Opioid receptors are involved in pain control, regulation of mood, reward, motivation, and response to stress. Four different types of opioid receptors have been identified: μ (OPRM), δ (OPRD), κ (OPRK), and the nociceptin (OPRX) receptor.[1] These receptors can be activated by endogeneous opioid peptides or exogenously administered opiates, which can act as analgesic drugs for severe pain. On the other hand, the binding of these ligands to the opioid receptors can result in other effects such as respiratory depression, euphoria, effects on mood, and inhibition of the gastrointestinal transit causing severe constipation and addiction. As a consequence, a straightforward goal of opiate research is the development of a drug lacking these undesirable side effects.[2]

Opioid receptors belong to the rhodopsin subclass within the superfamily of G-protein-coupled receptors (GPCRs).[3] These receptors are composed of a core domain of seven transmembrane α-helices (TM), connected by three intra- (IL) and three extracellular (EL) loops, and contain glycosylated N-terminal and palmitoylated C-terminal domains of variable lengths.[3−12] In the early 1990s, the human OPRM,[13] OPRD,[14,15] and OPRK[16−18] were cloned. Subtype protein sequences demonstrate high sequence homology in their TM (73−76%) and intracellular domains (63−66%). A large divergence exists in the N- and C-terminal domains and in the extracellular loops (34−40% identity).[19,20]

The use of X-ray diffraction analysis or NMR spectroscopy to directly evaluate receptor−ligand interactions is complicated by the fact that GPCRs are embedded in the cell membrane.[21] So far, crystal structures of rhodopsin (Rho)[4] and more recently opsin (Ops),[11] β-1 (ADRB1) and β-2 (ADRB2) adrenergic,[7−10] dopamine D3 (DRD3),[22] A2A adenosine,[12] and CXCR4 chemokine[23] receptors have been reported. For all other GPCRs, however, such crystallographic data are still absent and indirect experimental methods have to be applied in combination with in silico modeling techniques to locate key receptor−ligand interactions and construct three-dimensional receptor−ligand models.[24,25] In this way, site-directed mutagenesis studies, chimeric receptor studies, incorporation of metal binding sites, and analysis of ligand structure−affinity relationships have previously been used to investigate opioid receptor−ligand interactions.[16,26−33]

Received: March 28, 2011
Published: August 29, 2011

Such in silico studies can provide valuable insight into the binding mode of opioid ligands, in particular of flexible peptide ligands.[26] The use of conformational constraints to limit peptide flexibility has been proposed as a method to obtain information about the receptor-bound conformation from the preferred conformation,[34−37] based on the assumption that a change from the preferred conformation upon receptor binding has become energetically unfavorable. However, energetically unfavorable conformational rearrangements can be tolerated in some cases without penalizing the tightness of protein−ligand binding.[38] In the current study we have introduced conformationally constrained Phe analogues into opioid peptides and studied the binding mode of these analogues to the OPRM by molecular docking simulations. We show that opioid tetrapeptides with different (locally constrained) geometries can have a high affinity for OPRM by adopting different bound conformations in the receptor binding pocket. Interestingly, our studies suggest that the docked receptor bound ligand conformation can deviate from the low energy conformation of the unbound ligand as determined by solution NMR.[37]

Among the naturally occurring opioids, the heptapeptide dermorphin (H-Tyr-D-Ala-Phe-Gly-Tyr-Pro-Ser-NH_2), which was isolated from the skin of the South American frog *Phyllomedusa sauvagei*,[39] is one of the most potent and selective μ-opioid receptor agonists.[40] The minimal sequence required for opiate-like activity in vivo was shown to be the N-terminal tetrapeptide.[41,42] The replacement of Tyr^1 in opioid peptides with the unnatural amino acid 2′,6′-dimethyltyrosine (Dmt) increased their μ- or δ-opioid potency by 1 or 2 orders of magnitude.[43] H-Dmt-D-Ala-NH-$(CH_2)_3$-Ph was the first reported analogue of this type and was proven to be a potent but only moderately selective μ-agonist.[44] Subsequently, Dmt substitution yielded extraordinary potent and selective opioids such as [Dmt^1]DALDA (H-Dmt-D-Arg-Phe-Lys-NH_2),[45,46] [Dmt^1]TAPP (H-Dmt-D-Ala-Phe-Phe-NH_2),[47] and [Dmt^1]TIPP-NH_2 (H-Dmt-Tic-Phe-Phe-NH_2).[48] The opioid ligand DIPP-NH_2[Ψ] (H-Dmt-Ticψ(CH_2NH)Phe-Phe-NH_2) is an opioid μ agonist/δ antagonist that produces a potent analgesic effect, no physical dependence, and less tolerance than morphine in rats.[48]

Conformational restrictions in the flexibility of the peptide side chains have proven to cause shifts in selectivity and affinity. The use of β-methylated amino acids to bias the population of the χ_1 torsion angle has been pioneered by Hruby. Important effects on the receptor affinity, on selectivity, on the agonist or antagonist character, and on the duration of action have been observed in a variety of peptides,[34,35] including opioids.[49,50] Cyclization provides an alternative way to limit the flexibility of the side chain. The 4-amino-1,2,4,5-tetrahydro-2-benzazepin-3-one scaffold **1** (Aba, Figure 1) allows the side chain orientation of the Phe^3 residue to be fixed into the trans (χ_1 = 180°) or the gauche(+) (χ_1 = +60°) staggered conformations.[36,51]

Dermorphin, a μ-selective peptide ($IC_{50}{}^{\mu}$ = 2.4 nM, $IC_{50}{}^{\delta}$ = 295 nM),[51] loses its selectivity on incorporation of the conformationally constrained dipeptide [Aba-Gly] in positions 3 and 4, mainly by an increase in δ-affinity ($IC_{50}{}^{\mu}$ = 11.0 nM, $IC_{50}{}^{\delta}$ = 17.4 nM).[51] Introduction of the Hba **2** and Aba **1** scaffolds in positions 1 and 3, respectively, of the N-terminal tetrapeptides (H-Tyr-D-Ala-Phe-Gly-NH_2) of dermorphin does not dramatically change the μ affinity.[52] The δ affinity on the other hand is increased approximately by a factor of 100. Hence, the conformationally restricted tetrapeptides have a selectivity shifted toward OPRD. In a functional assay, however, the double constrained carboxamide tetrapeptide H-[Hba-D-Ala]-[Aba-Gly]-NH_2 ($IC_{50}{}^{\mu}$ = 20.8 nM) is the most potent agonist in the GPI (guinea pig ileum, IC_{50} = 3.64 nM) assay which contains mainly μ-opioid receptors. This peptide also shows potent in vivo antinociception after i.t. and iv administration and in addition possesses a prolonged duration of action.[52,53]

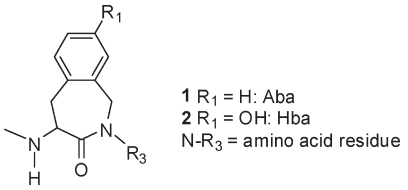

Figure 1. 4-Amino-1,2,4,5-tetrahydro-2-benzazepin-3-one **1** (Aba) and 8-hydroxy-4-amino-1,2,4,5-tetrahydro-2-benzazepin-3-one **2** (Hba) scaffolds.

We have recently reported that β-methylation of the Aba scaffold resulted in an unchanged ring and backbone conformation for both stereoisomers of (5*S*)- or (5*R*)-Me-Aba.[37] In contrast, α-methylation resulted in 4-Me-Aba which adopted a different ring conformation and induced a β-turn conformation in tetrapeptide models.[37] We have now investigated the effects of a combined introduction of the conformationally constrained Aba residue and of a methyl substituent in its 4- or 5-position in the opioid peptide H-Dmt-D-Ala-Phe-Gly-NH_2. A rationalization of the biological data by using the binding poses proposed by molecular docking simulations in OPRM will be presented.

RESULTS AND DISCUSSION

Synthesis. The synthesis of the Boc-protected *erythro*-(4*S*,5*S*) **3**, *erythro*-(4*R*,5*R*) **4**, *threo*-(4*S*,5*R*) **5**, and *threo*-(4*R*,5*S*)-Me-Aba-Gly-OH **6** building blocks (Figure 2) was performed as described for the racemates[37] using the corresponding enantiopure β-methylphenylalanine starting materials. Racemic *erythro*-β-MePhe and racemic *threo*-β-MePhe were *N*-Cbz protected and resolved by crystallization using quinine or quinidine according to the procedure of Kataoka.[54] Optical purity was determined after N-deprotection by chiral derivatization with Marfey's reagent N_α-(2,4-dinitro-5-fluorophenyl)-L-alaninamide (FDAA),[55] followed by HPLC analysis, which also allowed the confirmation of the absolute configuration of the samples.[56] After the formation of the benzazepinone ring,[37] the 5-methyl-Aba-Gly stereoisomers were *N*-Boc protected using Boc_2O and the resulting building blocks **3**−**6** were purified by crystallization as their dicyclohexylamine salts. In contrast to the *erythro* isomers **3** and **4**, the *threo* isomers **5** and **6** substantially epimerized during this procedure, which led to a contamination of **5** with **4** and of **6** with **3**. Fortunately, after peptide synthesis using these mixtures, the resulting diastereomeric peptides could be separated by reversed-phase preparative HPLC, and their configuration could be assigned by comparison with the peptides containing the enantiopure *erythro* isomers **3** and **4**.

In contrast to the 5-Me-substituted Aba-Gly stereoisomers, racemic H-(4*R*,*S*)-Me-Aba-Gly-OH was prepared using an earlier published strategy.[37] Briefly, racemic 2-amino-3-(2-cyanophenyl)-2-methylpropanoic acid was methyloxycarbonyl (Moc) protected, and the nitrile was reduced with H_2/10% Pd on C to provided the *o*-aminomethyl compound. Intramolecular cyclization using 1-ethyl-3-(3′-dimethylaminopropyl)carbodiimide (EDC) provided (*R*,*S*)-4-methyloxycarbonylamino-4-methyl-1,2,4,5- tetrahydro-2-benzazepin-3-one which was N-alkylated with *tert*-butyl

dx.doi.org/10.1021/jm2003574 |*J. Med. Chem.* 2011, 54, 6538–6547

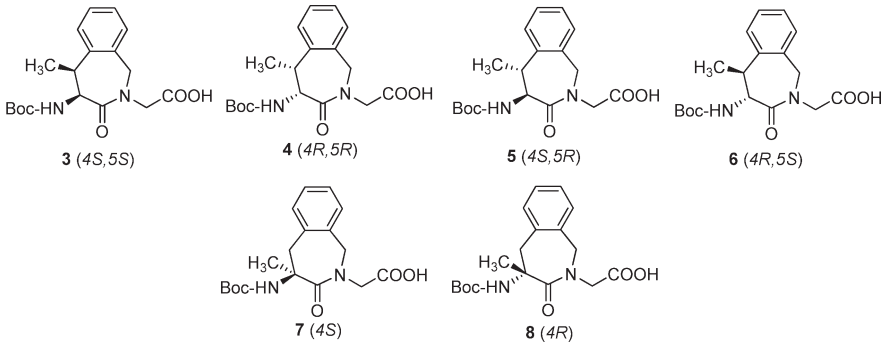

Figure 2. Boc-protected *erythro*-**3** (4*S*,5*S*) and **4** (4*R*,5*R*) and *threo*-5-Me-Aba-Gly-OH **5** (4*S*,5*R*) and **6** (4*R*,5*S*) and 4-Me-Aba-Gly-OH **7** (4*S*) and **8** (4*R*) building blocks.

Table 1. Constrained Tetrapeptide Analogues 9−16

H-Dmt-D-Ala-*erythro*-(4*S*,5*S*)-5-Me-Aba-Gly-NH_2 **9**
H-Dmt-D-Ala-*erythro*-(4*R*,5*R*)-5-Me-Aba-Gly-NH_2 **10**
H-Dmt-D-Ala-*threo*-(4*S*,5*R*)-5-Me-Aba-Gly-NH_2 **11**
H-Dmt-D-Ala-*threo*-(4*R*,5*S*)-5-Me-Aba-Gly-NH_2 **12**
H-Dmt-D-Ala-(4*S*)-Me-Aba-Gly-NH_2 **13**
H-Dmt-D-Ala-(4*R*)-Me-Aba-Gly-NH_2 **14**
H-Dmt-D-Ala-(4*S*)-Aba-Gly-NH_2 **15**
H-Dmt-D-Ala-(4*R*)-Aba-Gly-NH_2 **16**

bromoacetate and NaH as a base to Moc-(4*R*,*S*)-Me-Aba-Gly-O^{t}Bu. After Moc deprotection and ester hydrolysis in a 33% solution of HBr in AcOH, the compound was Boc-protected to Boc-(4*R*,*S*)-Me-Aba-Gly-OH. After incorporation into the tetrapeptide sequence the two epimeric peptides were separated by HPLC. To discriminate the (4*S*)- from the (4*R*)-isomer, an asymmetric synthesis of Boc-(4*S*)-Me-Aba-Gly-OH **7** (Figure 2) was required, which, after incorporation into the tetrapeptide, allowed the assignment of the (4*S*)-epimer by comparison of the HPLC retention times. Therefore, a small scale synthesis of (*S*)-α-methyl-*o*-cyanophenylalanine was performed by alkylation of the Schöllkopf chiral bislactim ether (2*R*,5*SR*)-2-isopropyl-3,6-dimethoxy-5-methyl-2,5-dihydropyrazine with *o*-cyanobenzyl bromide[57,58] and further transformation as described above for the racemate.[37]

Peptide Synthesis. Analogues **9**−**16** of the tetrapeptide H-Dmt-D-Ala-Phe-Gly-NH_2, containing the constrained building blocks **3**−**8** (Table 1), were prepared by solid-phase synthesis using Boc-chemistry and the 4-methylbenzhydrylamine resin as the solid support. Analogues **15** and **16** were prepared as reference ligands using Boc-(4*S*)-Aba-Gly-OH and Boc-(4*R*)-Aba-Gly-OH, respectively.[34] The target peptides were cleaved from the resin by HF_{liq} and purified by preparative high-performance liquid chromatography to a purity ≥95%.

Biological Evaluation: Receptor Binding Affinity and Functional Bioactivity. Receptor binding affinities of compounds **9**−**16** for OPRM and OPRD were determined by displacement of [^{3}H]DAMGO and [^{3}H][Ile^{5,6}]deltorphin-2 from rat brain membrane binding sites, respectively (Table 2). The in vitro activity of the ligands was tested in [^{35}S]GTPγS-binding experiments in rat brain membranes.[59]

The data in Table 2 indicate that all compounds have a higher affinity for OPRM than for OPRD. The affinities are much higher than those of the tyrosine-containing analogues,[52,53] which is consistent with the role of Dmt in opioid peptide analogues. Analogue **9** shows a very high μ-affinity and also a good δ-affinity, both of which are comparable to that of the unsubstituted reference compound **15**. Interestingly, analogue **12**, which has the *threo*-(4*R*,5*S*) configuration, exhibits a similar high affinity for OPRM, although it possesses an opposite absolute configuration at position 4 of the Aba ring. This is unusual, since in opioid peptides a D-configuration of residue 3 results in a decreased potency,[49,50,60,61] as is also the case for the (4*R*)-Aba-containing analogue **16**, compared to its (4*S*)-epimer **15**. A similar uncharacteristic observation was made for the α-methyl substituted analogues, for which compound **14**, having a (4*R*)-configuration at the α-carbon, is more potent than its (4*S*)-derivative **13**. The former of these has a similar affinity for the OPRM (K_i^{μ} = 0.3 nM) to the *erythro*-(4*R*,5*R*)-5-methyl isomer **10** (K_i^{μ} = 0.4 nM). Compound **10** is, however, more selective. All compounds show agonist properties in the [^{35}S]GTPγS-binding experiments with good potencies except for compounds **11** and **13**, which can be considered as low potency agonists, in agreement with their lower binding affinities.

Rationalization of the Biological Data by Molecular Docking Simulations to a OPRM Receptor Model. An attempt to explain the unexpected effects of the configuration at C-4 of the Aba residue in the tetrapeptide analogues was made by constructing a model for the OPRM and observing the binding poses of the ligands after automated docking. The recently solved ADRB2 crystal structure (PDB code 2RH1.pdb)[8] was used as a template to model the TM helices of the preliminary OPRM model, with the exception of TM2, which was derived from a previously reported CCR5 model[62] (the OPRM model was constructed before the release of the recently solved CXCR4 chemokine).[23] Arguments for this modeling template selection procedure are (i) the larger distance between TM3 and TM6 at the bottom of the ligand binding pocket in ADRB2 compared to the bovine rhodopsin crystal structure,[4,8] offering more space for docking the Dmt scaffold of the peptide ligands and (ii) the T2.56XP2.58 motif present in OPRM. This motif has been suggested to induce an alternative kink in TM2[63,64] compared to the rhodopsin and β adrenergic receptor crystal structures[4,8,10] and has been carefully modeled in the CCR5 template.[62] An extra turn of TM6 (6.56−6.58), derived from the ADRB2 crystal structure, was added to the preliminary model, locating lysine at position 6.58, which plays an important role in determining opioid receptor specificity,[65] into the binding pocket. The remainder of the procedure is described in the Experimental Section.

dx.doi.org/10.1021/jm2003574 |*J. Med. Chem.* 2011, 54, 6538–6547

Table 2. Binding Affinities and Functional Activities of Tetrapeptides 9−16

peptide	[^{3}H]DAMGO, K_i^μ (nM)	[^{3}H]Ile^{5,6} -deltorphin-2, K_i^δ (nM)	selectivity K_i^δ/K_i^μ (nM)	[^{35}S]GTPγS EC_{50}(nM)	[^{35}S]GTPγS E_{max} (%)
H-Dmt-D-Ala-[*erythro*-(4*S*,5*S*)-5-Me-Aba-Gly]-NH_2 **9**	0.025 ± 0.012	1.7 ± 0.9	68	36 ± 6	191 ± 11
H-Dmt-D-Ala-[*erythro*-(4*R*,5*R*)-5-Me-Aba-Gly]-NH_2 **10**	0.4 ± 0.08	490 ± 71	1225	184 ± 46	167 ± 3
H-Dmt-D-Ala-[*threo*-(4*S*,5*R*)-5-Me-Aba-Gly]-NH_2 **11**	14 ± 1.5	720 ± 109	51	685 ± 114	130 ± 3
H-Dmt-D-Ala-[*threo*-(4*R*,5*S*)-5-Me-Aba-Gly]-NH_2 **12**	0.025 ± 0.002	24 ± 6.4	960	9.3 ± 1.3	149 ± 3
H-Dmt-D-Ala-(4*S*)-4-Me-Aba-Gly-NH_2 **13**	4.6 ± 1.7	859 ± 107	187	941 ± 114	159 ± 1.2
H-Dmt-D-Ala-(4*R*)-4-Me-Aba-Gly-NH_2 **14**	0.3 ± 0.08	63 ± 1.5	210	288 ± 44	154 ± 10
H-Dmt-D-Ala-(4*S*)-Aba-Gly-NH_2 **15**	0.047 ± 0.012	2.4 ± 0.6	51	18 ± 6	161 ± 15
H-Dmt-D-Ala-(4*R*)-Aba-Gly-NH_2 **16**	0.33 ± 0.06	337 ± 28	1021	64.2 ± 2.1	178.2 ± 3.5

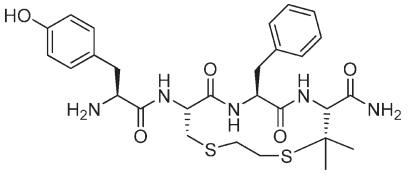

Figure 3. Tyr-c(S-Et-S)[D-Cys-Phe-D-Pen]NH_2 **17** (JOM-6).[24]

The starting point for the docking studies was the cyclic tetrapeptide **17** (JOM-6, Tyr-c(S-Et-S)[D-Cys-Phe-D-Pen]NH_2, Figure 3), which is a highly potent and selective agonist for OPRM (K_i = 0.17 nM) and for which binding poses in an OPRM model have been reported.[26]

The binding mode of the highest ranked Surflex, version 2.301,[66] docking pose of **17** in the OPRM receptor model (docking procedure described in the Experimental Section) is line with experimental data (Figure 4A).[26,27] The protonated amine group of the ligand forms a complementary H-bond interaction network with D3.32[28,29] and Y7.43,[30,31] while the Tyr^1 phenol ring binds in the hydrophobic pocket between Y3.33[30,32] and W6.48[32] and forms an H-bond with H6.52.[33] The Phe^3 group of **17** adopts a trans orientation[26] and forms an aromatic interaction with W7.35 in OPRM.[67] The C-terminal carboxamide group of **17** is in proximity of E5.35 in OPRM.[19,26]

Compounds **9**−**14** were docked into the refined OPRM receptor model with Surflex, version 2.301.[66] The best pose of **17** was used to generate a reference interaction fingerprint (IFP) as previously described,[68] and a Tanimoto coefficient (Tc-IFP) measuring IFP similarity with the reference **17** pose in the OPRM receptor model was used to filter and rank the docking poses of compounds **9**−**14**.

Docking poses of **9**, **11**, **12**, and **14** in the OPRM structure (see Figure 4A−C) involved in the same receptor−ligand interactions as **17**[26] (Figure 4A) were selected using a receptor−ligand interaction fingerprint (IFP) scoring method[68] as described earlier.[69] For high affinity compounds **9** and **12** and medium affinity compound **14** (but not for medium affinity compounds **10**, **11**, and **13**), poses could be found showing an ionic interaction with D3.32[28,29] as well as an H-bond to H6.52.[33] Figure 4 shows the top-ranked docking poses of **9** (Figure 4B), **11** (Figure 4C), **12** (Figure 4A−C), and **14** (Figure 4D) as well as a part of their receptor−ligand interaction fingerprint (IFP) bit strings (Figure 4E), compared to the experimentally supported[19,26,27] binding mode and IFP of **17** (Figure 4A,E). The N-terminal Dmt groups of high-affinity compounds **9** and **12** and medium affinity compound **14** form the same H-bond interactions with D3.32 and H6.52 as the N-terminal tyramine group of **17** and bind in the same hydrophobic pocket between Y3.33, F5.43, F5.47, and W6.48. The protonated nitrogen of medium affinity compound **11** is just out of H-bond distance (but within ionic interaction distance) to D3.32 but forms an H-bond with H6.52 as well (Figure 4C,E). The Aba group of high affinity compounds **9** and **12** stacks with W7.35 and H7.36, residues that play an important role in OPRM-specific agonist binding[67] (Figure 4A,B,D), and occupies the same binding pocket as the Phe3 ring of **17** between the top of TM7 and the second (G45.46 and F45.54) and third (T6.70) extracellular loops.[26] The 5-methyl group of **9** and **12** binds close to I7.39, a residue position critical for the selectivity of nociceptin receptor (T7.39 in wild-type) against opioid ligands,[70] and this interaction might be responsible for the increased affinity compared to the nonmethylated reference compound **15**. The C-terminal amide oxygen atom of these compounds forms an H-bond with the OPRM-specific residue K6.58 (like **17**). These data indicate that despite a different configuration at C-4 of the Aba ring, analogues **9** and **12** can adopt very similar binding poses, explaining their high affinity for the OPRM. For medium affinity compound **14** a different binding mode than for compounds **9**, **11**, and **12** was observed in which the Aba ring is stacking with the Dmt ring and is occupying the same space as the S-CH_2-CH_2-S bridge of **17** (Figure 4D). Interestingly, compound **14** is assumed to adopt a β-turn in solution by forming an intramolecular H-bond between the C-terminal carboxamide oxygen and the Ala backbone amide nitrogen atom.[37] Although compound **14** can adopt a β-turn in conformational searches (in line with previous ligand-based modeling studies,[37] results not shown), this β-turn conformation cannot be accommodated in the OPRM receptor model. In the proposed binding mode the C-terminal carboxamide group of **14** forms an intermolecular H-bond with K6.58 instead (Figure 4D). The predicted extended conformations of compounds **9**, **11**, and **12** are consistent with the NMR data on the preferred conformation of 5-Me-Aba tetrapeptide models.[37]

For medium/low affinity compounds **10** and **13** no docking poses were generated in which the Dmt group forms an ionic interaction with D3.32[28,29] and an H-bond with H6.52.[33] Comparison of the binding mode of **12** (Figure 4) and the ligand-based rapid overlay of chemical structures (ROCS)[71] of **10** and **13** with the docking pose of **12** (Figure 5) suggests that the conformations of the *erythro*-(4*R*,5*R*)-5-Me-Aba (**10**) (Figure 5A) and (4*S*)-Me-Aba (**13**) (Figure 5B) methyl groups do not properly match the shape of the OPRM specific binding pocket between W7.35 and H7.36.[67]

dx.doi.org/10.1021/jm2003574 |J. Med. Chem. 2011, 54, 6538–6547

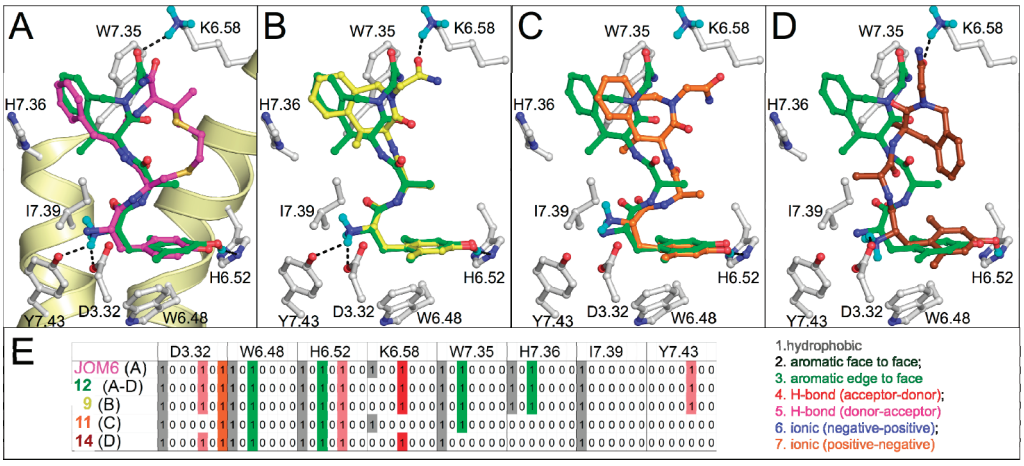

Figure 4. Docking poses selected by IFP of compounds **12** (A–D, green carbon atoms), **9** (B, yellow), **11** (C, orange), and **14** (D, brown) in the OPRM receptor model compared to the reference binding mode of **17** (A, magenta carbon atoms). Parts of the backbone of transmembrane (TM) helices 6 and 7 are represented by light yellow ribbons (TM3 and second (EL2) and third (EL3) extracellular loops are not shown for clarity). Important binding residues are depicted as ball-and-sticks with gray carbon atoms. Oxygen, nitrogen, sulfur, and hydrogen atoms are colored red, blue, orange, and cyan, respectively. H-bonds described in the text are depicted by black dots. The IFP bit strings of compounds **12** (A–D), **9** (B), **11** (C), and **14** (D) are compared to the reference IFP of **17** (A) in part E. For reasons of clarity, the bit strings of only eight residues (out of 26) are shown as an example.

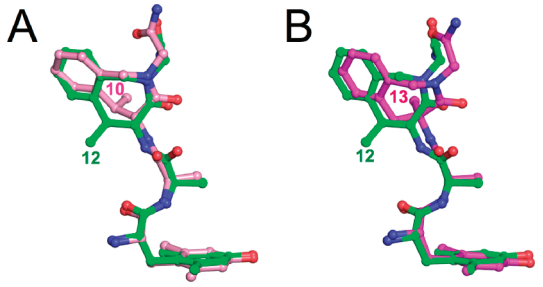

Figure 5. ROCS alignments of compound **10** (pink carbon atoms, A) and **13** (magenta, B) to the docking pose of compound **12** (green). The rendering and visual orientation are the same as in Figure 4. Misaligned methyl groups are indicated by the corresponding compound number.

The structure–activity relationships and molecular docking studies of our conformationally restricted tetrapeptides indicate that in addition to recognition of an aromatic amine and aromatic moiety between TM3 (D3.32, Y3.33), TM6 (W6.48, H6.52), and TM7 (Y7.43), a tight steric fit of the ligand in the hydrophobic binding pocket between W7.35 and H7.36 (two residues that play an important role in OPRM-specific agonist binding[67]) is essential for high OPRM affinity. We therefore propose targeting this binding pocket with apolar moieties as a general design strategy for OPRM ligands.

CONCLUSIONS

Several of the tetrapeptides synthesized in this study are high affinity OPRM agonist with selectivity over the OPRD. Interesting effects of the Aba configuration on ligand binding affinity were rationalized by molecular docking simulations of the opioid tetrapeptides in a three-dimensional OPRM receptor model. Compounds **9** and **12** have subnanomolar affinity for OPRM, although they possess an opposite absolute configuration at position 4 of Aba, while compound **14** was significantly more potent than its (4*S*)-stereoisomer **13**. Our docking studies predict that high affinity OPRM ligands can form similar interactions within the receptor binding pocket by adopting different conformations and support the idea that OPRM bound ligand conformations can deviate from low energy *unbound* ligand conformations.

EXPERIMENTAL SECTION

General Methods. RP-HPLC was performed using a RP C-18 column (Supelco Discovery BIO Wide Pore C18, l = 25 cm, d = 0.45 cm, PS = 5 μm) with a mobile phase consisting of water/acetonitrile containing 0.1% TFA. Products were eluted using the following parameters: gradient, t = 0 min, 3% CH_3CN, t = 20 min, 97% CH_3CN; flow rate, 1.0 mL min^{-1}; λ = 215 nm. Preparative HPLC was performed using a RP C-18 column (Supelco Discovery BIO Wide Pore C18, l = 25 cm, d = 2.12 cm, PS = 10 μm) with the above-mentioned gradient at a flow rate of 20.0 mL min^{-1}. TLC analysis was performed on plastic sheets precoated with silica gel 60F_{254} (Merck). Melting points were measured with a Büchi B 540 melting point apparatus, with a temperature increment of 1 °C min^{-1}. ^{1}H and ^{13}C NMR spectra were recorded at 250.13 and 62.90 MHz, respectively, with a Bruker Avance DRX250 spectrometer, using TMS or the residual solvent signal as internal reference. For some advanced NMR analyses samples were measured with the Bruker AMX500 spectrometer, using pulse sequences of the Bruker program library. Mass spectra were recorded on a VG Quattro II spectrometer using electrospray ionization (positive ion mode). The MBHA resin was purchased from Neosystem (Strasbourg, France). Boc-Dmt-OH was obtained from RSP Amino Acids (Shirley, MA). 2-1*H*-(Benzotriazol-1-yl)-1,1,3,3-tetramethyluronium tetrafluoroborate (TBTU) was purchased from Senn Chemicals (Dielsdorf, Switzerland).

Synthetic Procedures. For the synthesis of Boc-protected *erythro*-(4*S*,5*S*)- (**3**), *erythro*-(4*R*,5*R*)- (**4**), *threo*-(4*S*,5*R*)- (**5**), and *threo*-(4*R*,5*S*)-5-Me-Aba-Gly-OH (**6**), see Supporting Information.

Peptide Synthesis. The N-terminal tetrapeptides **9**–**16** were prepared through solid-phase synthesis using Boc chemistry and the MBHA resin (0.95 mmol/g) as solid support. A 3-fold excess of the amino acids and coupling reagent (TBTU) was used together with a 9-fold excess of the base NMM and a 1:1 mixture of dry DMF/dry CH_2Cl_2 was used as a solvent system. Final cleavage of the peptide from the resin was done by treatment with HF_{liq} for 1 h at 0 °C (2 mL of anisole and 10 mL of HF_{liq} were applied for 1 g of peptide–resin). These crude mixtures were purified by preparative HPLC, and the pure

dx.doi.org/10.1021/jm2003574 |*J. Med. Chem.* 2011, 54, 6538–6547

peptides were isolated as their TFA salt with purities of ≥95% as determined by analytical HPLC and TLC using the conditions mentioned above (see General Methods).

H-Dmt-D-Ala-[*erythro*-(4*S*,5*S*)-5-Me-Aba-Gly]-NH_2·TFA 9. Preparative HPLC yielded the desired compound (white powder, 31%). HPLC (standard gradient): t_R = 10.8 min. TLC R_f(EBAW) = 0.69. HRMS (ESP+) MW $C_{27}H_{35}N_5O_5$·TFA = 623.6 g/mol. Found m/z 510.2701 $[M + H]^+$, $C_{27}H_{36}N_5O_5$ (without TFA) requires 510.2711.

H-Dmt-D-Ala-[*erythro*-(4*R*,5*R*)-5-Me-Aba-Gly]-NH_2·TFA 10. Preparative HPLC yielded the desired compound (white powder, 71%). HPLC (standard gradient): t_R = 10.3 min. TLC R_f(EBAW): 0. 54. HRMS (ESP+) MW $C_{27}H_{35}N_5O_5$·TFA = 623.6 g/mol. Found m/z 510.2711 $[M + H]^+$, $C_{27}H_{36}N_5O_5$ (without TFA) requires 510.2711.

H-Dmt-D-Ala-[*threo*-(4*S*,5*R*)-5-Me-Aba-Gly]-NH_2·TFA 11. Preparative HPLC yielded the desired compound (white powder, 23% + 19%: erythro-(4*R*,5*R*)-derivative **10**). HPLC (standard gradient): t_R = 10.4 min. TLC R_f(EBAW) = 0.70. HRMS (ESP+) MW $C_{27}H_{35}N_5O_5$·TFA = 623.6 g/mol. Found m/z 510.2705 $[M + H]^+$, $C_{27}H_{36}N_5O_5$ (without TFA) requires 510.2711.

H-Dmt-D-Ala-[*threo*-(4*R*,5*S*)-5-Me-Aba-Gly]-NH_2·TFA 12. Preparative HPLC yielded the desired compound (white powder, 22% + 28% *erythro*-(4*S*,5*S*)-derivative **9**). HPLC (standard gradient): t_R = 10.9 min. TLC R_f(EBAW): 0. 69. HRMS (ESP+) MW $C_{27}H_{35}N_5O_5$·TFA = 623.6 g/mol. Found m/z 510.2711 $[M + H]^+$, $C_{27}H_{36}N_5O_5$ (without TFA) requires 510.2711.

H-Dmt-D-Ala-[(4*S*)-Me-Aba-Gly]-NH_2·TFA 13. Preparative HPLC yielded the desired compound (white powder, 25%). HPLC (standard gradient): t_R = 10.3 min. TLC R_f(EBAW) = 0.71. HRMS (ESP+) MW $C_{27}H_{35}N_5O_5$·TFA = 623.6 g/mol. Found m/z 510.2695 $[M + H]^+$, $C_{27}H_{36}N_5O_5$ (without TFA) requires 510.2711.

H-Dmt-D-Ala-[(4*R*)-Me-Aba-Gly]-NH_2·TFA 14. Preparative HPLC yielded the desired compound (white powder, 21%). HPLC (standard gradient): t_R = 11.0 min. TLC R_f(EBAW) = 0.71. HRMS (ESP+) MW $C_{27}H_{35}N_5O_5$·TFA = 623.6 g/mol. Found m/z 510.2720 $[M + H]^+$, $C_{27}H_{36}N_5O_5$ (without TFA) requires 510.2711.

H-Dmt-D-Ala-(4*S*)-Aba-Gly-NH_2·TFA 15. Preparative HPLC yielded the desired compound (white powder, 38%). HPLC (standard gradient): t_R = 10.1 min. TLC R_f(EBAW) = 0.65. HRMS (ESP+) MW $C_{26}H_{33}N_5O_5$·TFA = 609.3 g/mol. Found m/z 496.2545 $[M + H]^+$, $C_{26}H_{34}N_5O_5$ (without TFA) requires 496.2554.

H-Dmt-D-Ala-(4*R*)-Aba-Gly-NH_2·TFA 16. Preparative HPLC yielded the desired compound (white powder, 41%). HPLC (standard gradient): t_R = 9.7 min. TLC R_f(EBAW) = 0.56. HRMS (ESP+) MW $C_{26}H_{33}N_5O_5$·TFA = 609.3 g/mol. Found m/z 496.2550 $[M + H]^+$, $C_{26}H_{34}N_5O_5$ (without TFA) requires 496.2554.

Radioligand Binding Assay. For competitive binding experiments, rat brain membrane homogenates (Wistar, male, 250−300 g body weight) were used, which were prepared as described by Bozü et al.[72] The protein content of the homogenates was determined by the method of Bradford[73] using BSA as a standard. The protein concentration was varied between 0.2 and 0.4 mg/test tube. The following conditions were set to assess inhibitory constants: [^{3}H]DAMGO (25 °C, 1 h, GF/C filter, glass tube), [^{3}H]Ile^{5,6}deltorphin-2 (35 °C, 45 min, GF/B filter, plastic tube, 0.25 mg of BSA/tube). The incubation mixtures were made up to a final volume of 1 mL with 50 mM Tris-HCl buffer (pH 7.4), and samples were incubated in a shaking water bath at the appropriate temperature. Competition binding experiments were performed by incubating the membranes with 0.5 nM [^{3}H]DAMGO, 2 nM [^{3}H]Ile^{5,6}deltorphin-2, and increasing concentrations (10^{-11}−10^{-5} M) of unlabeled dermorphin analogues. Nonspecific binding was determined with 10 μM naloxone and subtracted from the total binding to yield the specific binding. Incubation was initiated by the addition of the membrane suspension and stopped by rapid filtration over Whatman GF/C or GF/B glass fiber filters, using a Brandel cell harvester. Filters were washed with 3 × 5 mL of ice-cold Tris-HCl buffer (pH 7.4), and then the filter-bound radioactivity was measured in an Optiphase Supermix scintillation cocktail (Perkin-Elmer) by immersing the filters in the cocktail, using a TRI-CARB 2100TR liquid scintillation counter. Each experiment was performed in duplicate and analyzed by the one/two-site binding competition fitting option of the GraphPad Prism software.

Ligand-Stimulated [^{35}S]GTPγS Functional Assay. Rat brain membranes (15 μg of protein/tube) were incubated with 0.05 nM [^{35}S]GTPγS and 10^{-10}−10^{-5} M opioids in the presence of 30 μM GDP, 100 mM NaCl, 3 mM $MgCl_2$, and 1 mM EGTA in 50 mM Tris-HCl pH 7.4 buffer for 60 min at 30 °C. Basal binding was measured in the absence of opioids and was corrected for the nonspecific binding to yield the specific binding. Nonspecific binding was determined with 10 μM unlabeled GTPγS. The reaction was initiated by the addition of the protein and terminated by the addition of 5 mL of ice-cold buffer (50 mM Tris-HCl, pH 7.4) to the vials and filtering the samples through a Whatman GF/B glass fiber filter with a Brandel cell harvester. Vials were washed three times with 5 mL of ice-cold buffer and then directly immersed in an Optiphase Supermix scintillation cocktail. The radioactivity was measured using a TRI-CARB 2100TR liquid scintillation counter. Ligand stimulations were expressed as percentage of the specific [^{35}S]GTPγS binding over the basal activity. Each measurement was performed in triplicate and analyzed by the sigmoid dose−response curve fitting option of the GraphPad Prism software.

Homology Modeling and Automated Docking. In order to get agonist-bound models of the OPRM receptor, we mainly followed a previously defined five-step protocol.[69]

The recently solved ADRB2 crystal structure[7−9] (PDB code 2RH1.pdb)[8] was used as template to model the TM helices of the preliminary OPRM model, with the exception of TM2, which was derived from a previously validated CCR5 model.[62] The Ballesteros−Weinstein residue numbering[24] scheme was used throughout this work for GPCR TM helices, while a recently proposed numbering[69] scheme was used to number the residues in the second extracellular loop (EL2). An extra turn of TM6 (6.56−6.58), derived from the ADRB2 crystal structure, was added to the preliminary model because position 6.58 plays an important role in determining opioid receptor specificity.[65]

This preliminary high-throughput receptor model was generated using the GPCRgen program.[74] The amino acid sequence alignments used for constructing the receptor models are shown in Supporting Information Figure 1.

In the second step, the known cyclic peptide agonist **17** was docked into this preliminary model using Surflex, version 2.301.[66] The trans ring conformation of **17**[19,26,75] was chosen as input for the docking simulations. Experimentally driven H-bond constraints were used to preliminarily guide the docking process in the OPRM receptor (1) between the protonated amine of Tyr^1 of **17** and both D3.32[28,29] carboxylate oxygen atoms, (2) between the hydroxyl group of Tyr^1 of **17** and the Nε2 hydrogen atom of H6.52,[33] (3) between the C-terminal carboxamide nitrogen of **17** and the carboxylate group of E5.35.[19,26]

In the third step, the agonist−receptor complex was minimized with AMBER 8[76] using the AMBER 03 force field to relax the structure and remove steric bumps. The minimizations were performed by 1000 steps of steepest descent followed by conjugate gradient until the rms gradient of the potential energy was lower than 0.05 kcal/(mol·Å). A twin cutoff (12.0 and 15.0 Å) was used to calculate nonbonded electrostatic interactions, and the nonbonded pair list was updated every 25 steps.

In the fourth step, a five-residue window around C45.50 was added to the TM model by threading this part of EL2 onto the bRho crystal structure and changing the residues in the respective residues of the OPRM receptor. The rest of EL2 was constructed using two subsequent Modeller 9v1[77] runs with explicit disulfide bridge constraints (between C3.25 in TM3 and C45.50 in EL2) and including the agonist binding

pose in the TM template as "block" residue. In the first run, the bovine rhodopsin crystal structure (PDB code 1U19.pdb)[6] was used to model the part upstream of EL2. Out of the 15 generated models, the model with the highest Modeller and DOPE scores and EL2 loop conformations properly accommodating the original agonist binding orientation in the original TM model was selected as input for a second Modeller run. In this second run, the EL2 segment downstream from the β_4 sheet was constructed. One out of 15 models was again selected based on the criteria described before. For the modeling of the EL2 of OPRM, additional upper-bound distance constraints, based on experimental data,[26] were defined between the OD1 atom of D45.49 and the ND1 atom of H7.35 (3.5 Å) and the Phe3 of **17** and the CA atom of G45.46 (5.0 Å).

After optimization of the EL2 conformation, extracellular loops 1 and 3, intracellular loops 1, 2, and 3, and helix 8 were modeled based on the bovine rhodopsin crystal structure (PDB code 1U19.pdb)[6] using Modeller 9v1.[77] The N-terminus and C-terminus were not included in any of the models. The final receptor model was energy minimized with the initially minimized agonist docking pose as described before.

In the final step, the full agonist−receptor complex was embedded in a pre-equilibrated lipid bilayer consisting of 77 (OPRM) molecules of 1-palmitoyl-2-oleoylphosphatidylcholine (POPC) and solvated with 9215 (OPRM) TIP3P water molecules (box dimensions of 82.8 Å × 79.4 Å × 81.5 Å (OPRM)) as described by Urizar et al.[78] A short minimization was applied to the complex embedded in the hydrated lipid bilayer using AMBER 8 and applying a positional harmonic constraint of 50 kcal/(mol·Å) on Cα carbon atoms. The entire system was then subjected to a 500 ps constant pressure molecular dynamics (MD) simulation. All bonds involving hydrogen atoms were frozen with the SHAKE algorithm. During the first 250 ps, the Cα carbon atoms were constrained as previously described and the temperature was linearly increased from 0 to 300 K. During the last 250 ps, the temperature was kept constant at 300 K and 1 bar, using a coupling constant of 0.2 and the Berendsen approach. Interactions were calculated according to the AMBER 03 force field, using particle mesh Ewald (MPE) summation to include the long-range electrostratic forces. van der Waals interactions were calculated using a cutoff of 8.0 Å. The same upper-bound distance restraints defined for the EL2 Modeller runs were also used during the MD simulations. Agonist force field parameters were derived using the Antechamber program,[74] and partial charges for the substrates were derived using the AM1-BCC procedure in Antechamber.

Molecular dynamics snapshots were clustered with the GROMACS g_cluster tool with respect to TM Cα atoms and according to the Jarvis−Patrick method, using a cutoff of 1.0 Å for defining the nearest neighbor. This yielded four (OPRM) clusters per simulation run. The cluster representative snapshots were subjected to a short energy minimization as described above, and the "best" snapshot was chosen to conduct the subsequent docking studies on. The "best" snapshot was chosen based on its ability to accommodate **17** in a binding mode in line with experimental data[26,27] by unconstrained docking with Surflex, version 2.301[66] (Figure 4A).

Compounds **9**−**14** were docked using standard parameters of Surflex, version 2.301.[66] **17** was used to generate reference interaction fingerprints (IFPs) as previously described.[68] Seven different interaction types (negatively charged, positively charged, H-bond acceptor, H-bond donor, aromatic face-to-edge, aromatic face-to-face, and hydrophobic interactions) were used to define the IFP. The cavity used for the IFP analysis consisted of the 26 residues within 4 Å distance from **17** in the refined receptor−ligand complex: D3.32, Y3.33, F3.37, G45.46, S45.47, D45.49, C45.50, T45.51, L45.52, T45.53, F45.54, H45.56, E5.35, K5.39, F5.43, F5.47, W6.48, I6.51, H6.52, V6.55, K6.58, T6.70, W7.35, H7.36, I7.39, Y7.43. Standard IFP scoring parameters[68] and a Tanimoto coefficient (Tc-IFP) measuring IFP similarity with the reference **17** pose in the OPRM receptor model were used to filter (only poses forming an ionic interaction with D3.32 and H-bond interaction with H6.52 are considered) and rank the docking poses of compounds **9**−**14**. For compounds **10** and **13** no docking poses were generated in which the Dmt group forms an ionic interaction with D3.32[28,29] and an H-bond with H6.52.[33] These compounds were therefore aligned with the selected docking pose of compound **12** using ROCS, version 2.3.1.[71] The conformer databases of compounds **10** and **13** were generated using standard settings of OMEGA, version 2.2.1,[79] and the best alignments of **10** and **13** with **12** were selected based on Comboscore (combination of shape Tanimoto and the normalized color score in this optimized overlay).[71]

■ ASSOCIATED CONTENT

Supporting Information. Synthesis protocol and characterization of **3**−**6**, amino acid alignments of transmembrane helices and intra- and extracellular loops, and full IFP bit strings of **9**, **11**, **12**, and **14**. This material is available free of charge via the Internet at http://pubs.acs.org.

■ AUTHOR INFORMATION

Corresponding Author

*For C.d.G: (address) Leiden/Amsterdam Center for Drug Research, Division of Medicinal Chemistry, Faculty of Science, VU University Amsterdam, De Boelelaan 1083, 1081 HV Amsterdam, The Netherlands; (phone) +31 20 5987550; (e-mail) C.de.Graaf@few.vu.nl. For D.T.: (phone) +32 2 6293295, (e-mail) datourwe@vub.ac.be.

■ ACKNOWLEDGMENT

The authors thank the Fund for Scientific Research Flanders (FWO-Vlaanderen), the EU Grant Normolife LSHC-CT-2006-037733, and AstraZeneca for financial support. S.B. is a postdoctoral fellow of the FWO-Vlaanderen.

■ ABBREVIATIONS USED

Aba, 4-amino-1,2,4,5-tetrahydro-2-benzazepin-3-one; Boc, *tert*-butyloxycarbonyl; BSA, bovine serum albumin; Cbz, benzyloxycarbonyl; DAMGO, H-Tyr-D-Ala-Gly-NMePhe-Gly-ol; Dmt, 2′,6′-dimethyltyrosine; EBAW, 1:1:1:1 ethyl acetate/*n*-butanol/acetic acid/water; EL, extracellular loop; FDAA, N_α-(2,4-dinitro-5-fluorophenyl)-L-alaninamide; GDP, guanosine 5′-diphosphate; GTPγS, guanosine 5′-*O*-(3-thio)triphosphate; GPCR, G-protein-coupled receptor; GPI, guinea pig ileum; IFP, interaction fingerprint; IL, intracellular loop; Ile^{5,6}-deltorphin-2, H-Tyr-D-Ala-Phe-Glu-Ile-Ile-Gly-NH_2; i.t., intrathecal; iv, intravenous; JOM-6, Tyr-c(S-Et-S)[D-Cys-Phe-D-Pen]NH_2; MBHA, 4-methylbenzhydrylamine; βMePhe, β-methylphenylalanine; OPRD, δ opioid receptor; OPRK, κ opioid receptor; OPRM, μ opioid receptor; OPRX, nociceptin receptor; Pen, β,β-dimethylcysteine or penicilamine; ROCS, rapid overlay of chemical structures; TFA, trifluoroacetic acid; TLC, thin layer chromatography; TM, transmembrane; TMS, tetramethylsilane

■ REFERENCES

(1) Kieffer, B. L. Opioid receptors: from genes to mice. *J. Pain* **2000**, *1*, 45–50.

(2) Eguchi, M. Recent advances in selective opioid receptor agonists and antagonists. *Med. Res. Rev.* **2004**, *24*, 182–212.

(3) Lagerström, M. C.; Schiöth, H. B. Structural diversity of G protein-coupled receptors and significance for drug discovery. *Nat. Rev. Drug Discovery* **2008**, *7*, 339–357.
(4) Palczewski, K.; Kumasaka, T.; Hori, T.; Behnke, C. A.; Motoshima, H.; Fox, B. A.; Le Trong, I.; Teller, D. C.; Okada, T.; Stenkamp, R. E.; Yamamoto, M.; Miyano, M. Crystal structure of rhodopsin: a G protein-coupled receptor. *Science* **2000**, *289*, 739–745.
(5) Okada, T.; Ernst, O. P.; Palczewski, K.; Hofmann, K. P. Activation of rhodopsin: new insights from structural and biochemical studies. *Trends Biochem. Sci.* **2001**, *26*, 318–324.
(6) Li, J.; Edwards, P. C.; Burghammer, M.; Villa, C.; Schertler, G. F. X. Structure of bovine rhodopsin in a trigonal crystal form. *J. Mol. Biol.* **2004**, *343*, 1409–1438.
(7) Rosenbaum, D. M.; Cherezov, V.; Hanson, M. A.; Rasmussen, S. G. F.; Thian, F. S.; Kobilka, T. S.; Choi, H. J.; Yao, X. J.; Weis, W. I.; Stevens, R. C.; Kobilka, B. K. GPCR engineering yields high-resolution structural insights into beta(2)-adrenergic receptor function. *Science* **2007**, *318*, 1266–1273.
(8) Cherezov, V.; Rosenbaum, D. M.; Hanson, M. A.; Rasmussen, S. G. F.; Thian, F. S.; Kobilka, T. S.; Choi, H. J.; Kuhn, P.; Weis, W. I.; Kobilka, B. K.; Stevens, R. C. High-resolution crystal structure of an engineered human beta(2)-adrenergic G protein-coupled receptor. *Science* **2007**, *318*, 1258–1265.
(9) Rasmussen, S. G. F.; Choi, H. J.; Rosenbaum, D. M.; Kobilka, T. S.; Thian, F. S.; Edwards, P. C.; Burghammer, M.; Ratnala, V. R. P.; Sanishvili, R.; Fischetti, R. F.; Schertler, G. F. X.; Weis, W. I.; Kobilka, B. K. Crystal structure of the human beta(2) adrenergic G-protein-coupled receptor. *Nature* **2007**, *450*, 383–3U4.
(10) Warne, T.; Serrano-Vega, M. J.; Baker, J. G.; Moukhametzianov, R.; Edwards, P. C.; Henderson, R.; Leslie, A. G. W.; Tate, C. G.; Schertler, G. F. X. Structure of a beta(1)-adrenergic G-protein-coupled receptor. *Nature* **2008**, *454*, 486–491.
(11) Scheerer, P.; Park, J. H.; Hildebrand, P. W.; Kim, Y. J.; Krauss, N.; Choe, H. W.; Hofmann, K. P.; Ernst, O. P. Crystal structure of opsin in its G-protein-interacting conformation. *Nature* **2008**, *455*, 497–502.
(12) Jaakola, V. P.; Griffith, M. T.; Hanson, M. A.; Cherezov, V.; Chien, E. Y. T.; Lane, J. R.; Ijzerman, A. P.; Stevens, R. C. The 2.6 Å crystal structure of a human A2A adenosine receptor bound to an antagonist. *Science* **2008**, *322*, 1211–1217.
(13) Wang, J. B.; Johnson, P. S.; Persico, A. M.; Hawkins, A. L.; Griffin, C. A.; Uhl, G. R. Human mu-opiate receptor: cDNA and genomic clones, pharmacological characterization and chromosomal assignment. *FEBS Lett.* **1994**, *338*, 217–222.
(14) Knapp, R. J.; Malatynska, E.; Fang, L.; Li, X. P.; Babin, E.; Nguyen, M.; Santoro, G.; Varga, E. V.; Hruby, V. J.; Roeske, W. R.; Yamamura, H. I. Identification of a human delta-opioid receptor: cloning and expression. *Life Sci.* **1994**, *54*, L463–L469.
(15) Simonin, F.; Befort, K.; Gaveriauxruff, C.; Matthes, H.; Nappey, V.; Lannes, B.; Micheletti, G.; Kieffer, B. The human delta-opioid receptor: genomic organization, cDNA cloning, functional expression, and distribution in human brain. *Mol. Pharmacol.* **1994**, *46*, 1015–1021.
(16) Simonin, F.; Gaveriauxruff, C.; Befort, K.; Matthes, H.; Lannes, B.; Micheletti, G.; Mattei, M. G.; Charron, G.; Bloch, B.; Kieffer, B. Kappa-opioid receptor in humans: cDNA and genomic cloning, chromosomal assignment, functional expression, pharmacology, and expression pattern in the central-nervous-system. *Proc. Natl. Acad. Sci. U.S.A.* **1995**, *92*, 7006–7010.
(17) Mansson, E.; Bare, L.; Yang, D. M. Isolation of a human kappa-opioid receptor cDNA from placenta. *Biochem. Biophys. Res. Commun.* **1994**, *202*, 1431–1437.
(18) Zhu, J. M.; Chen, C. G.; Xue, J. C.; Kunapuli, S.; Deriel, J. K.; Liuchen, L. Y. Cloning of a human kappa-opioid receptor from the brain. *Life Sci.* **1995**, *56*, L201–L207.
(19) Pogozheva, I. D.; Przydzial, M. J.; Mosberg, H. I. Homology modeling of opioid receptor−ligand complexes using experimental constraints. *AAPS J.* **2005**, *7*, E434–E448.
(20) Chen, Y.; Mestek, A.; Liu, J.; Yu, L. Molecular-cloning of a rat kappa-opioid receptor reveals sequence similarities to the mu-opioid and delta-opioid receptors. *Biochem. J.* **1993**, *295*, 625–628.
(21) Cherezov, V.; Abola, E.; Stevens, R. C. Recent progress in the structure determination of GPCRs, a membrane protein family with high potential as pharmaceutical targets. *Methods Mol. Biol.* **2010**, *654*, 141–168.
(22) Chien, E. Y.; Liu, W; Zhao, Q; Katritch, V; Han, G. W.; Hanson, M. A.; Shi, L; Newman, A. H.; Javitch, J. A.; Cherezov, V; Stevens, R. C. Structure of the human dopamine D3 receptor in complex with a D2/D3 selective antagonist. *Science* **2010**, *330*, 1091–1095.
(23) Wu, B.; Chien, E. Y.; Mol, C. D.; Fenalti, G.; Liu, W.; Katritch, V.; Abagyan, R.; Brooun, A.; Wells, P.; Bi, F. C.; Hamel, D. J.; Kuhn, P.; Handel, T. M.; Cherezov, V.; Stevens, R. C. Structures of the CXCR4 chemokine GPCR with small-molecule and cyclic peptide antagonists. *Science* **2010**, *330*, 1066–1071.
(24) Ballesteros, J. A.; Shi, L.; Javitch, J. A. Structural mimicry in G-protein-coupled receptors: implications of high-resolution structure of rhodopsin for structure−function analysis of rhodopsin-like receptors. *Mol. Pharmacol.* **2001**, *60*, 1–19.
(25) de Graaf, C.; Rognan, D. Customizing G protein-coupled receptor models for structure-based virtual screening. *Curr. Pharm. Des.* **2009**, *15*, 4026–4048.
(26) Fowler, C. B.; Pogozheva, I. D.; Lomize, A. L.; LeVine, H.; Mosberg, H. I. Complex of an active mu-opioid receptor with a cyclic peptide agonist modeled from experimental constraints. *Biochemistry* **2004**, *43*, 15796–15810.
(27) Fowler, C. B.; Pogozheva, I. D.; LeVine, H.; Mosberg, H. I. Refinement of a homology model of the mu-opioid receptor using distance constraints from intrinsic and engineered zinc-binding sites. *Biochemistry* **2004**, *43*, 8700–8710.
(28) Li, J. G.; Chen, C. G.; Yin, J. L.; Rice, K.; Zhang, Y.; Matecka, D.; de Riel, J. K.; DesJarlais, R. L.; Liu-Chen, L. Y. Asp147 in the third transmembrane helix of the rat mu opioid receptor forms ion-pairing with morphine and naltrexone. *Life Sci.* **1999**, *65*, 175–185.
(29) Surratt, C. K.; Johnson, P. S.; Moriwaki, A.; Seidleck, B. K.; Blaschak, C. J.; Wang, J. B.; Uhl, G. R. Mu opiate receptor: charged transmembrane domain amino-acids are critical for agonist recognition and intrinsic activity. *J. Biol. Chem.* **1994**, *269*, 20548–20553.
(30) Befort, K.; Tabbara, L.; Kling, D.; Maigret, B.; Kieffer, B. L. Role of aromatic transmembrane residues of the delta-opioid receptor in ligand recognition. *J. Biol. Chem.* **1996**, *271*, 10161–10168.
(31) Befort, K.; Zilliox, C.; Filliol, D.; Yue, S. Y.; Kieffer, B. L. Constitutive activation of the delta opioid receptor by mutations in transmembrane domains III and VII. *J. Biol. Chem.* **1999**, *274*, 18574–18581.
(32) Xu, H.; Lu, Y. F.; Partilla, J. S.; Zheng, Q. X.; Wang, J. B.; Brine, G. A.; Carroll, F. I.; Rice, K. C.; Chen, K. X.; Chi, Z. Q.; Rothman, R. B. Opioid peptide receptor studies, 11: Involvement of Tyr148, Trp318 and His319 of the rat mu-opioid receptor in binding of mu-selective ligands. *Synapse* **1999**, *32*, 23–28.
(33) Spivak, C. E.; Beglan, C. L.; Seidleck, B. K.; Hirshbein, L. D.; Blaschak, C. J.; Uhl, G. R.; Surratt, C. K. Naloxone activation of mu-opioid receptors mutated at a histidine residue lining the opioid binding cavity. *Mol. Pharmacol.* **1997**, *52*, 983–992.
(34) Hruby, V. J. Design in topographical space and peptidomimetic ligands that affect behavior. A chemist's glipse at the mind−body problem. *Acc. Chem. Res.* **2001**, *34*, 389–397.
(35) Hruby, V. J. Organic chemistry and biology: chemical biology through the eyes of collaboration. *J. Org. Chem.* **2009**, *74*, 9245–9264.
(36) Tourwé, D.; Verschueren, K.; Frycia, A.; Davis, P.; Porreca, F.; Hruby, V. J.; Toth, G.; Jaspers, H.; Verheyden, P.; VanBinst, G. Conformational restriction of Tyr and Phe side chains in opioid peptides: information about preferred and bioactive side-chain topology. *Biopolymers* **1996**, *38*, 1–12.
(37) De Wachter, R.; Brans, L.; Ballet, S.; Van den Eynde, I.; Urbanczyk-Lipkovska, Z.; Tourwe, D. Influence of ring substitutions on the conformation and β-turn mimicry of 4-amino-1,2,4,5-tetrahydro-2-benzazepin-3-one peptide mimetics. *Tetrahedron* **2009**, *65*, 2266–2278.
(38) Perola, E.; Charifson, E. Conformational analysis of drug-like molecules bound to proteins: an extensive study of ligand reorganization upon binding. *J. Med. Chem.* **2004**, *47*, 2499–510.

(39) Montecucchi, P. C.; Henschen, A. Amino-acid-composition and sequence-analysis of sauvagine, a new active peptide from the skin of *Phyllomedusa sauvagei*. *Int. J. Pept. Protein Res.* **1981**, *18*, 113–120.

(40) Amiche, M.; Sagan, S.; Mor, A.; Delfour, A.; Nicolas, P. Characterization of the receptor-binding profile of (H-3) dermorphin in the rat-brain. *Int. J. Pept. Protein Res.* **1988**, *32*, 506–511.

(41) Broccardo, M.; Erspamer, V.; Falconierierspamer, G.; Improta, G.; Linari, G.; Melchiorri, P.; Montecucchi, P. C. Pharmacological data on dermorphins, a new class of potent opioid-peptides from amphibian skin. *Br. J. Pharmacol.* **1981**, *73*, 625–631.

(42) Melchiorri, P.; Negri, L. The dermorphin peptide family. *Gen. Pharmacol.* **1996**, *27*, 1099–1107.

(43) Bryant, S. D.; Jinsmaa, Y.; Salvadori, S.; Okada, Y.; Lazarus, L. H. Dmt and opioid peptides: a potent alliance. *Biopolymers* **2003**, *71*, 86–102.

(44) Chandrakumar, N. S.; Yonan, P. K.; Stapelfeld, A.; Savage, M.; Rorbacher, E.; Contreras, P. C.; Hammond, D. Preparation and opioid activity of analogs of the analgesic dipeptide 2,6-dimethyl-L-tyrosyl-*N*-(3-phenylpropyl)-D-alaninamide. *J. Med. Chem.* **1992**, *35*, 223–233.

(45) Schiller, P. W.; Weltrowska, G.; Schmidt, R.; Nguyen, T. M. D.; Berezowska, I.; Chen, Y.; Lemieux, C.; Chung, N. N.; Wilkes, B. C.; Carpenter, K. A. Opioid Peptide Analogs with Novel Activity Profiles as Potential Therapeutic Agents for Use in Analgesia. In *Peptide Science: Present and Future*, Proceedings of the 1st International Peptide Symposium, Kyoto, Japan, Dec 1997; Shimonishi, Y., Ed.; Kluwer Academic Publishers: Dordrecht, The Netherlands, 1999; pp 665−669.

(46) Schiller, P. W.; Nguyen, T. M. D.; Berezowska, I.; Dupuis, S.; Weltrowska, G.; Chung, N. N.; Lemieux, C. Synthesis and in vitro opioid activity profiles of DALDA analogues. *Eur. J. Med. Chem.* **2000**, *35*, 895–901.

(47) Berezowska, I.; Lemieux, C.; Nguyen, T. M. D.; Chung, N. N.; Schiller, P. W. Opioid Peptide Analogs Containing 2′-Hydroxy, 6′-Methyltyrosine in Place of Tyr1 Display Greatly Enhanced δ Agonist Potency but Unchanged μ Agonist Potency. In *Peptides 1998*, Proceedings of the 25th European Peptide Symposium, Budapest, Hungary; Bajusz, S., Hudecz, F., Eds.; Akadémiai Kiadó: Budapest, Hungary, 1998; pp 718−719.

(48) Schiller, P. W.; Fundytus, M. E.; Merovitz, L.; Weltrowska, G.; Nguyen, T. M.-D.; Lemieux, C.; Chung, N. N.; Coderre, T. J. The opioid μ agonist/δ antagonist DIPP-$NH_2[\psi]$ produces a potent analgesic effect, no physical dependence, and less tolerance than morphine in rats. *J. Med. Chem.* **1999**, *42*, 3520–526.

(49) Tourwé, D.; Mannekens, E.; Nguyen Thi Diem, T.; Verheyden, P.; Jaspers, H.; Tóth, G.; Péter, A.; Kertész, I.; Török, G.; Chung, N. N.; Schiller, P. W. Side chain methyl substitution in the delta-opioid receptor antagonist TIPP has an important effect on the activity profile. *J. Med. Chem.* **1998**, *41*, 5167–5176.

(50) Tömböly, Cs.; Köver, K. E.; Péter, A.; Tourwé, D.; Biyashev, D.; Benyhe, S.; Borsodi, A.; Al-Khrasani, M.; Ronai, A. Z.; Tóth, G. Structure−activity study on the Phe side chain arrangement of endomorphins using conformationally constrained analogues. *J. Med. Chem.* **2004**, *47*, 735–743.

(51) Tourwé, D.; Verschueren, K.; Van Binst, G.; Davis, P.; Porreca, F.; Hruby, V. J. Dermorphin sequence with high delta-affinity by fixing the Phe side-chain to trans at χ1. *Bioorg. Med. Chem. Lett.* **1992**, *2*, 1305–1308.

(52) Ballet, S.; Frycia, A.; Piron, J.; Chung, N. N.; Schiller, P. W.; Kosson, P.; Lipkowski, A. W.; Tourwe, D. Synthesis and biological evaluation of constrained analogues of the opioid peptide H-Tyr-D-Ala-Phe-Gly-NH_2 using the 4-amino-2-benzazepin-3-one scaffold. *J. Pept. Res.* **2005**, *66*, 222–230.

(53) Ballet, S.; Misicka, A.; Kosson, P.; Lemieux, C.; Chung, N. N.; Schiller, P. W.; Lipkowski, A. W.; Tourwe, D. Blood−brain barrier penetration by two dermorphin tetrapeptide analogues: role of lipophilicity vs structural flexibility. *J. Med. Chem.* **2008**, *51*, 2571–2574.

(54) Kataoka, Y.; Seto, Y; Yamamoto, M. Studies of unusual amino-acids and their peptides. 6. Synthesis and optical resolutions of beta-methylphenylalanine and its dipeptide present in bottromycin. *Bull. Chem. Soc. Jpn.* **1976**, *46*, 1081–1084.

(55) Marfey, P. Determination of D-amino acids. 2. Use of a bifunctional reagent, 1,5-difluoro-2,4-dinitrobenzene. *Carlsberg Res. Commun.* **1984**, *49*, 591–596.

(56) Péter, J.; Tóth, G.; Török, G.; Tourwé, D. Separation of enantiomeric β-methyl amino acids and of β-methyl amino acid containing peptides. *J. Chromatogr., A* **1996**, *728*, 455–465.

(57) Vassiliou, S.; Magriotis, P. A. Improved Schöllkopf construction of quaternary alpha-amino acids: efficient enantioselective synthesis of integrin LFA-1 antagonist BIRT-377. *Tetrahedron: Asymmetry* **2006**, *17*, 1754–1757.

(58) Vandormael, B.; De Wachter, R.; Martins, J. C.; Hendrickx, P. M. S.; Keresztes, A.; Ballet, S.; Mallaredy, J. R.; Tóth, F.; Tóth, G.; Tourwé, D. Asymmetric synthesis and conformational analysis by NMR spectroscopy and MD of Aba- and α-MeAba-containing dermorphin analogues. *ChemMedChem* [Online early access]. DOI: 10.1002/cmdc.201100314. Published Online: Aug 29, **2011**.

(59) Traynor, J. R.; Nahorski, S. R. Modulation by mu-opioid agonists of guanosine-5′-*O*-(3-[S-35]thio)triphosphate binding to membranes from human neuroblastoma Sh-Sy5y cells. *Mol. Pharmacol.* **1995**, *47*, 848–854.

(60) Darlak, K.; Grzonka, Z.; Krascik, P.; Janicki, P.; Gumulka, S. W. Structure−activity studies of dermorphin. The role of side chains of amino acid residues on the biological activity of dermorphin. *Peptides* **1984**, *5*, 687–689.

(61) Misicka, A.; Cavagnero, S.; Horvath, R.; Davis, P.; Porreca, F.; Yamamura, H. I.; Hruby, V. J. Synthesis and biological properties of β-$MePhe^3$ analogues of deltorphin I and dermenkephalin: influence of biased χ1 of Phe3 residues on peptide recognition for δ-opioid receptors. *J. Pept. Res.* **1997**, *50*, 48–54.

(62) Kellenberger, E.; Springael, J. Y.; Parmentier, M.; Hachet-Haas, M.; Galzi, J. L.; Rognan, D. Identification of nonpeptide CCR5 receptor agonists by structure-based virtual screening. *J. Med. Chem.* **2007**, *50*, 1294–1303.

(63) Govaerts, C.; Bondue, A.; Springael, J. Y.; Olivella, M.; Deupi, X.; Le Poul, E.; Wodak, S. J.; Parmentier, M.; Pardo, L.; Blanpain, C. Activation of CCR5 by chemokines involves an aromatic cluster between transmembrane helices 2 and 3. *J. Biol. Chem.* **2003**, *278*, 1892–1903.

(64) Govaerts, C.; Blanpain, C.; Deupi, X.; Ballet, S.; Ballesteros, J. A.; Wodak, S. J.; Vassart, G.; Pardo, L.; Parmentier, M. The TXP motif in the second transmembrane helix of CCR5. A structural determinant of chemokine-induced activation. *J. Biol. Chem.* **2001**, *276*, 13217–13225.

(65) Valiquette, M.; Vu, H. K.; Yue, S. Y.; Wahlestedt, C.; Walker, P. Involvement of Trp-284, Val-296, and Val-297 of the human delta-opioid receptor in binding of delta-selective ligands. *J. Biol. Chem.* **1996**, *271*, 18789–18796.

(66) Jain, A. N. Surflex-Dock 2.1: robust performance from ligand energetic modeling, ring flexibility, and knowledge-based search. *J. Comput.-Aided Mol. Des.* **2007**, *21*, 281–306.

(67) Bonner, G.; Meng, F.; Akil, H. Selectivity of mu-opioid receptor determined by interfacial residues near third extracellular loop. *Eur. J. Pharmacol.* **2000**, *403*, 37–44.

(68) Marcou, G.; Rognan, D. Optimizing fragment and scaffold docking by use of molecular interaction fingerprints. *J. Chem. Inf. Model.* **2007**, *47*, 195–207.

(69) de Graaf, C.; Foata, N.; Engkvist, O.; Rognan, D. Molecular modeling of the second extracellular loop of G-protein coupled receptors and its implication on structure-based virtual screening. *Proteins* **2008**, *71*, 599–620.

(70) Owens, C. E.; Akil, H. Determinants of ligand selectivity at the κ-receptor based on the structure of the orphanin FQ receptor. *J. Pharmacol. Exp. Ther.* **2002**, *300*, 992–999.

(71) *ROCS*, version 2.3.1; OpenEye Scientific Software: Santa Fe, NM; www.eyesopen.com.

(72) Bozü, B.; Fülöp, F.; Toth, G. K.; Toth, G.; Szücs, M. Synthesis and opioid binding activity of dermorphin analogues containing cyclic beta-amino acids. *Neuropeptides* **1997**, *31*, 367–372.

(73) Bradford, M. M. A rapid and sensitive method for the quantitation of microgram quantities of protein utilizing the principle of protein−dye binding. *Anal. Biochem.* **2008**, *72*, 248–254.

(74) Bissantz, C.; Logean, A.; Rognan, D. High-throughput modeling of human G-protein coupled receptors: amino acid sequence alignment, three-dimensional model building, and receptor library screening. *J. Chem. Inf. Comput. Sci.* **2004**, *44*, 1162–1176.

(75) Mosberg, H. I.; Fowler, C. B. Development and validation of opioid ligand−receptor interaction models: the structural basis of mu vs. delta selectivity. *J. Pept. Res.* **2002**, *60*, 329–335.

(76) Wang, J. M.; Wolf, R. M.; Caldwell, J. W.; Kollman, P. A.; Case, D. A. Development and testing of a general AMBER force field. *J. Comput. Chem.* **2004**, *25*, 1157–1174.

(77) Sali, A.; Blundell, T. L. Comparative protein modeling by satisfaction of spatial restraints. *J. Mol. Biol.* **1993**, *234*, 779–815.

(78) Urizar, E.; Claeysen, S.; Deupi, X.; Govaerts, C.; Costagliola, S.; Vassart, G.; Pardo, L. An activation switch in the rhodopsin family of G protein-coupled receptors. The thyrotropin receptor. *J. Biol. Chem.* **2005**, *280*, 17135–17141.

(79) *OMEGA*, version 2.2.1; OpenEye Scientific Software: Santa Fe, NM; www.eyesopen.com.